International Journal of Hybrid Information Technology
Vol. 9, No.12 (2016), pp. 343-356
http://dx.doi.org/10.14257/ijhit.2016.9.12.31

Workspace and Structural Parameter Analysis for a Novel 3-PRS Parallel Mechanism

Fuwei Sun, Junwei Zhao and Guoqiang Chen

(School of Mechanical and Power Engineering, Henan Polytechnic University, Jiaozuo 454003, China)
hpusfw2016@sina.com

Abstract

The working space is one of the important indexes to measure the working capability of parallel mechanism. In this paper, the working space of a new type of 3-PRS parallel mechanism is studied. In the beginning, a novel 3-PRS parallel mechanism is proposed with the kinematics analyzed, and then the working space and volume are obtained by search algorithm, and the working space is drawn using MATLAB. Finally, the influence of the structural parameters on the working space is discussed, which provide theoretical basis for parameter optimization.

***Keywords**: 3-PRS parallel mechanism; constraint; workspace; structural parameter.*

1. Introduction

The parallel mechanism has a wide range of application on the practical engineering such as aerospace, micro manufacturing and so on, thanks to the characteristics of high rigidity, small inertia, small accumulated error and compact structure. For example, 6 degrees of freedom Stewart parallel mechanism has been widely used in aerospace and industrial production [1].Since the appearance of parallel mechanism with few degrees of freedom (less than 6 degrees of freedom), it has also become a hot research topic, and the results of this research have been achieved [2-4]. However, there are many technical issues to be resolved, such as design and manufacturing accuracy of structural components, complex control, working space, positive solutions, etc. Working space is an important measure to evaluate the performance of parallel mechanism which directly reflects the working capacity. Besides of that, it is also an important foundation for parallel mechanism design, motion planning, scale synthesis and so on. [5, 6].For different organizations, there are many kinds of research methods to design and optimize the parallel mechanism, such as algebraic method, numerical method, random search method, and so on[7-12].Kang Jian-li et al. [13] used the Monte Carlo method to describe the working space of the 3-PRS mechanism, Lei Jing-tao [14] analyzed the workspace of 4UPS-UP parallel mechanism using boundary search method, and Ji ye et al. [15]calculated dimensional size of position workspace and scope of attitude workspace in the solution of different scale using the set of points. In this paper, a new type of 3-PRS parallel mechanism is introduced, and the working space and characteristics are obtained by using the search algorithm in different conditions, which has important significance for the optimization design of 3-PRS parallel mechanism.

ISSN: 1738-9968 IJHIT

2. Mechanism Model and Inverse Kinematics Analysis

2.1. Summary of 3-PRS Parallel Mechanism

The schematic diagram of the 3-PRS parallel mechanism is shown in Figure 1, and structural parameters are listed in Table 1. The 3-PRS parallel mechanism comprises cutter, fixed platform and moving platform, three horizontal guide rails with 120° distribution $A_iB_i (i=1,2,3)$, three vertical slides P_iD_i （$i=1,2,3$） and three identical branched chains P_iS_i （$i=1,2,3$） .The cutter is mounted vertically in the center of the moving platform, and each branched chain contains a connecting rod, a prismatic pair (P), a Revolute (R) and a spherical pair (S).The fixed coordinate system $O-XYZ$ is located on the static platform. Axis OX at the point A_1, and center O is the midpoint of the A_1A_2.The dynamic coordinate system O^T-xyz is located on the moving platform. Center O^T is located at the tip (or shaft end), and axis O^Tx at the point S_1.Axis O^Tz along the axis of the spindle.

R is circumradius of $A_1A_2A_3$, which is located on the inside of the horizontal guide rail. r is circumradius of $S_1S_2S_3$, which is located on the moving platform. H_i is the height of P_iD_i. θ_i （$i=1,2,3$） is the included angle between P_iS_i and P_iD_i. h is the distance between the tip and the center of the moving platform. R_i is the distance between the slider D_i and the center of the pedestal O'.

The 3-PRS parallel machine structure with adjustable working space has 3 degrees of freedom that are around X, Y axis rotation and movement along the Z axis, which is different from the common parallel mechanism, and the three sliding blocks on the base can be adjusted. In the practical application, the working space of the 3-PRS parallel mechanism can be changed by adjusting the position of the sliding block on the horizontal guide rail.

Table 1. Structure Parameters of 3-PRS Parallel Mechanism

Name	r	R	l	h	H	R_i
Value/mm	150	350	820	120	$0\le H\le 900$	$350\le R_i\le 600$

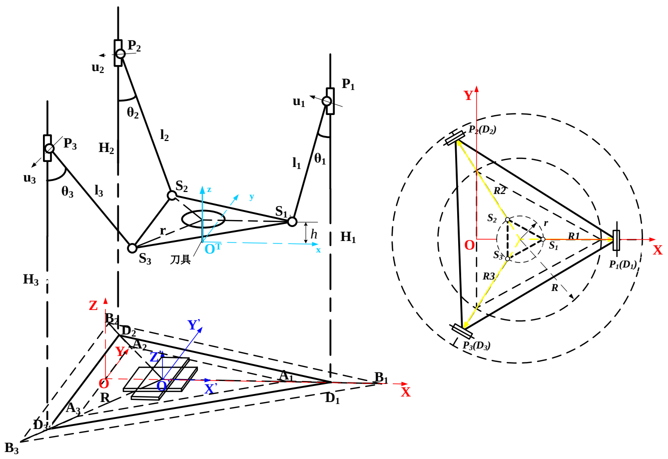

Figure 1. The Diagram of the Series-parallel Machine Structure with Adjustable Working Space

2.2. Inverse Kinematics Analysis of 3-PRS Parallel Mechanism

Correspondingly, the inverse kinematics analysis of the 3-PRS parallel mechanism is that the position and attitude parameters of the end effector are known, and the position parameters of the vertical sliding block are solved. In the fixed coordinate system $O-XYZ$, the vector displacement of D_i and P_i are as follows:

$$\begin{aligned} \overrightarrow{D_1} &= \left[R_1+\frac{R}{2},0,0\right]^T \\ \overrightarrow{D_2} &= \left[\frac{R-R_2}{2},\frac{\sqrt{3}}{2}R_2,0\right]^T \\ \overrightarrow{D_3} &= \left[\frac{R-R_3}{2},-\frac{\sqrt{3}}{2}R_3,0\right]^T \end{aligned} \tag{1}$$

$$\begin{aligned} \overrightarrow{P_1} &= \left[R_1+\frac{R}{2},0,H_1\right]^T \\ \overrightarrow{P_2} &= \left[\frac{R-R_2}{2},\frac{\sqrt{3}}{2}R_2,H_2\right]^T \\ \overrightarrow{P_3} &= \left[\frac{R-R_3}{2},-\frac{\sqrt{3}}{2}R_3,H_3\right]^T \end{aligned} \tag{2}$$

In dynamic coordinate system O^T-xyz, the vector displacement of S_i is as follows:

$$\begin{aligned} \overrightarrow{S_1} &= \left[r,0,h\right]^T \\ \overrightarrow{S_2} &= \left[-\frac{1}{2}r,\frac{\sqrt{3}}{2}r,h\right]^T \\ \overrightarrow{S_3} &= \left[-\frac{1}{2}r,-\frac{\sqrt{3}}{2}r,h\right]^T \end{aligned} \tag{3}$$

In dynamic coordinate system O^T-xyz, the vector displacement of O^T is as follows:

$$\overrightarrow{O^T} = \left[x_T,y_T,z_T\right]^T \tag{4}$$

The transition matrix $[T]$ of moving coordinate system with respect to fixed coordinate system is as follows:

$$[T]=\begin{bmatrix} k_1 & m_1 & n_1 \\ k_2 & m_2 & n_2 \\ k_3 & m_3 & n_3 \end{bmatrix}$$
$$\begin{bmatrix} \cos\beta\cos\gamma & -\cos\beta\sin\gamma & \sin\beta \\ \sin\alpha\sin\beta\cos\gamma+\cos\alpha\sin\gamma & -\sin\alpha\sin\beta\sin\gamma+\cos\alpha\cos\gamma & -\sin\alpha\cos\beta \\ \sin\alpha\sin\gamma-\cos\alpha\sin\beta\cos\gamma & \sin\alpha\cos\gamma+\cos\alpha\sin\beta\sin\gamma & \cos\alpha\cos\beta \end{bmatrix} \tag{5}$$

where, α,β,γ are the rotation angles which around the X, Y and Z axes in the moving coordinate system. The displacement of spherical hinge S_i can be expressed as follows in the fixed coordinate system $O-XYZ$.

$$\left[S_i\right]_{OXYZ} = \left[T\right]\left[S_i\right]_{oxyz} + O^T, i=1,2,3 \tag{6}$$

Equation (3), (4) and (5) into Equation (6), the displacement of spherical hinge S_i in the fixed coordinate system $O-XYZ$ is rewritten:

$$\overrightarrow{S_1^o} = \begin{bmatrix} rk_1 + hn_1 + x_T \\ rk_2 + hn_2 + y_T \\ rk_3 + hn_3 + z_T \end{bmatrix} \tag{7}$$

$$\overrightarrow{S_2^o} = \begin{bmatrix} -\frac{1}{2}rk_1 + \frac{\sqrt{3}}{2}rm_1 + hn_1 + x_T \\ -\frac{1}{2}rk_2 + \frac{\sqrt{3}}{2}rm_2 + hn_2 + y_T \\ -\frac{1}{2}rk_3 + \frac{\sqrt{3}}{2}rm_3 + hn_3 + z_T \end{bmatrix} \tag{8}$$

$$\overrightarrow{S_3^o} = \begin{bmatrix} -\frac{1}{2}rk_1 - \frac{\sqrt{3}}{2}rm_1 + hn_1 + x_T \\ -\frac{1}{2}rk_2 - \frac{\sqrt{3}}{2}rm_2 + hn_2 + y_T \\ -\frac{1}{2}rk_3 - \frac{\sqrt{3}}{2}rm_3 + hn_3 + z_T \end{bmatrix} \tag{9}$$

Each connecting rod can move only in the corresponding space plane because of constraint of Revolute, and the expression for the constraint space plane is as follows:

$$\Omega_1 : Y = 0$$

$$\Omega_2 : Y = -\sqrt{3}\left(X - \frac{1}{2}R \right)$$

$$\Omega_3 : Y = \sqrt{3}\left(X - \frac{1}{2}R \right)$$

Equations (7), (8), (9) into the constraint equation, as follows can be obtained.

$$\begin{cases} rk_2 + hn_2 + y_T = 0 \\ -\frac{1}{2}rk_2 + \frac{\sqrt{3}}{2}rm_2 + hn_2 + y_T = -\sqrt{3}(-\frac{1}{2}rk_1 + \frac{\sqrt{3}}{2}rm_1 + hn_1 + x_T - \frac{1}{2}R_2) \\ -\frac{1}{2}rk_2 - \frac{\sqrt{3}}{2}rm_2 + hn_2 + y_T = \sqrt{3}(-\frac{1}{2}rk_1 + \frac{\sqrt{3}}{2}rm_1 + hn_1 + x_T - \frac{1}{2}R_2) \end{cases} \tag{10}$$

Simplify Equation (10),it would become:

$$\begin{cases} r = f(\alpha, \beta) = -\arctan(\frac{\sqrt{3}R_2 - \sqrt{3}R_3 + 6r\sin\alpha\sin\beta}{6r\cos\alpha + 6r\cos\beta}) \\ x_T = \frac{1}{2}r(\cos\beta\cos\gamma + \sin\alpha\sin\beta\sin\gamma - \cos\alpha\cos\gamma) - h\sin\beta + \frac{1}{4}R_2 + \frac{1}{4}R_3 \\ y_T = h\sin\alpha\cos\beta - r\sin\alpha\sin\beta\cos\gamma - r\cos\alpha\sin\gamma \end{cases} \tag{11}$$

Equations (11) indicates that the parameter γ depends on α and β, and x_T, y_T are functions of α, β, r, h and $R_i (i = 1,2,3)$ .Given z_T, α and β, the position of the spherical hinge S_i can be obtained by Equations (7), (8), (9) in the fixed coordinate system $O-XYZ$. The length of the connecting rod is fixed, and the position component of the movable pair on the Z axis can be determined by the following type:

$$H_i = \sqrt{l_i^2 - (P_{iX} - S_{iX})^2 - (P_{iY} - S_{iY})^2} + S_{iZ}, i = 1, 2, 3 \tag{12}$$

3. Workspace Analysis

3.1. Main Constraints on the Working Space of the Mechanism

(1) Constraint of slide block

The base of the 3-PRS parallel mechanism can be adjusted, and the sliding block can move along the horizontal guide rail. Its adjustable range is $R_{\min} \le R_i \le R_{\max} (i = 1,2,3)$.

(2) Constraint of vertical sliding stroke

The vertical slider moves up and down along the vertical guide rail, and it is restricted by the length of the guide rail, the structure size of the connecting rod and the cutter, and the sliding block can move only within a certain range. The guide rail structure and the lead of each sliding block are identical. $H_{\min}$ is the minimum displacement. Correspondingly $H_{\max}$ is the maximum displacement. The constraint condition for the slide stroke is $H_{\min} \le H_i \le H_{\max} (i = 1,2,3)$.

(3) Interference constraint of connecting rod

The moving platform is connected with the sliding block through a connecting rod together with a certain size. There may be interference between the connecting rod when the robot is working. In order to avoid the occurrence of interference, the angle between the connecting rod and the moving platform is more than 180°, that is, the following conditions are satisfied:

$$(\overrightarrow{P_1S_1} \times \overrightarrow{S_1S_0}) \times \vec{j} > 0$$
$$(\overrightarrow{P_2S_2} \times \overrightarrow{S_2S_0}) \times \vec{i} > 0$$
$$(\overrightarrow{P_3S_3} \times \overrightarrow{S_3S_0}) \times \vec{j} > 0$$

where, $\vec{i}$ and $\vec{j}$ are the unit vector of the x axis and y axis in the moving coordinate system $O^T - xyz$. S_0 represents the geometric center of the moving platform. $\overrightarrow{P_iS_i} \times \overrightarrow{S_iS_0}$ indicates the direction vector of the plane of P_iS_i and S_iS_0.

(4) Constraint of Rotation angle

The connecting rod and the sliding block are connected by Revolute, and the rotation angle is in a certain range. In the mechanism, the rotation angle range is $0^\circ < \theta_i < 60^\circ$.

3.2. Example Analysis and the Influence of Key Parameters on Working Space

3.2.1. Example Analysis

The working space of the 3-PRS parallel mechanism is a set of attitude angles that can be achieved at different heights when the center of the moving platform is moving along a straight line, and the mechanism is constrained by the block stroke, the vertical sliding stroke, the interference between connecting rod and Rotation angle, then, the working space of the mechanism is in line with the working area of these constraints. The search algorithm is used to calculate these regions, and the basic steps are as follows:

(1) The end position coordinates (x_T, y_T, z_T) of the moving platform are determined as the target search space, and the space is divided into several sub spaces with a thickness of Δz by family of planes with parallel to xoy plane.

(2) the end position coordinates (x_T, y_T, z_T) of the moving platform are searched according to the constraints which are given in each subspace starting from $z = 0$.

(3) after the completion of a sub space of the search, an investigation for a subspace of Δz is performed again, until $z = z_{\max}$. $z_{\max}$ is the highest point of the working space that is allowed by the constraint conditions. The end position coordinates of the moving platform of each subspace are searched out, and the space combination is the working space of the mechanism.

In order to describe the size of the working space more clearly, the volume of working space is introduced, and its calculation is as follows:

$$V = \sum V_i = \sum A_i \Delta z \tag{13}$$

Where, V_i is the volume of the sub space. A_i is the area of the subspace projection on the xoy surface. Δz is the height of the sub space.

In this example, the parameters of the structure are shown in Table 2, and the working space of the mechanism is searched by MATLAB. Figure 2 describing the graphic model of workspace shows that, the working space is the symmetry in the z axis, and the upper part of the work space is a cone and the lower part of the workspace is column with constant cross-section. Figure 3 is the projection of the working space on the xoy surface when $z = 640$, $z = 680$, $z = 720$, $z = 760$. It can be concluded from Figure 3 that the working space is symmetrical, and the section outline of the working space is gradually reduced with the increase of center height of the moving platform in the z axis .That shows that the posture ability of the moving platform is gradually reduced.

Table 2. The Parameters of the Structure

Name	R_1	R_2	R_3	r	h	l_1	l_2	l_3
Value	350	350	350	150	20	820	820	820

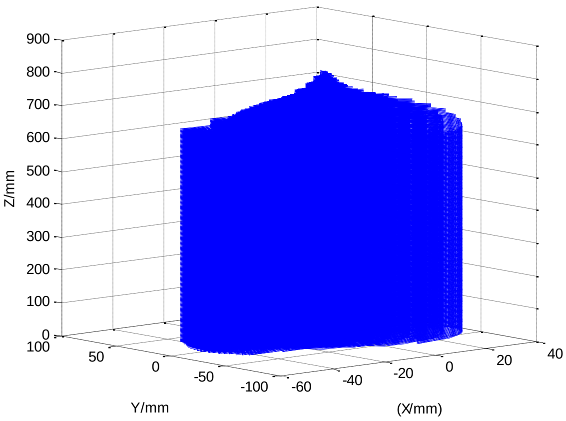

Figure 2. The Working Space of the 3-PRS Parallel Mechanism

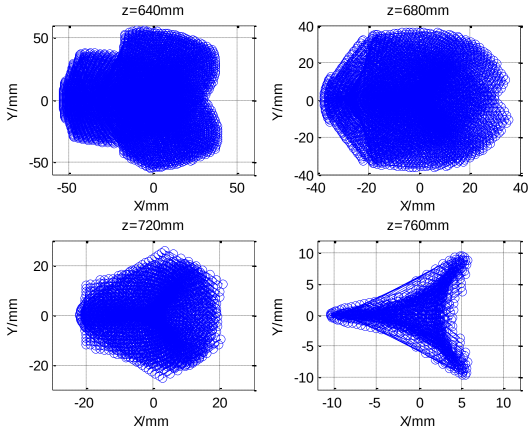

Figure 3. The Working Space Projection on the xoy Surface

3.2.2. The Influence of Key Parameters on Working Space

In the 3-PRS parallel mechanism, the base radius R and the length l of the connecting rod can be changed within a certain range. The paper mainly studies the influence of R and l on the working space, and this provides a theoretical basis for the optimization design of the mechanism.

Influence of base radius R on working space. The parameters of the mechanism are as follows: $r = 150mm$, $l_i = 820mm$ （$i = 1,2,3$） , $h = 20mm$. $R_1 = R_2 = R_3$, R values for 350mm, 400mm, 450mm and 500mm. Table 3 shows the working space width on the x axis and y axis, the working space height on the z axis and the volume of the working space. Figure 4-Figure 8 show the working space nephogram and projection on xoy, xoz and yoz surfaces.

Table 3. Influence of Base Radius R on Working Space

R (mm)	350	400	450	500
working space width on the x axis (mm)	86. 5031	86.5031	78. 9523	38. 5563
working space width on the y axis (mm)	114.8175	114.8175	92.0645	50.4084
working space height on the z axis (mm)	807	792	775	753
volume of the working space (mm^3)	5. 2597× 10^6	5.1153× 10^6	3. 6640× 10^6	0.90256× 10^6

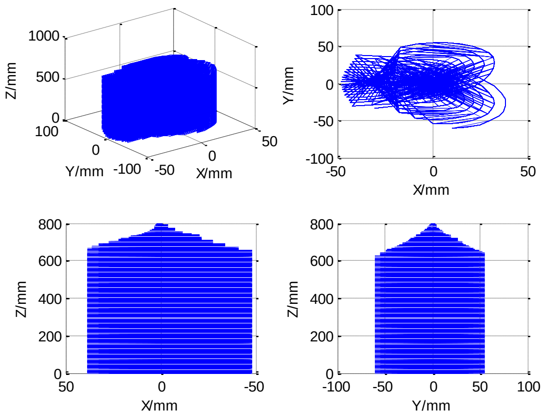

Figure 4. Working Space in $R=350mm$

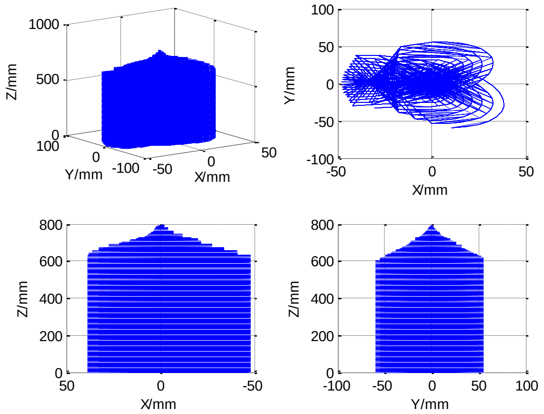

Figure 5. Working Space in $R=400mm$

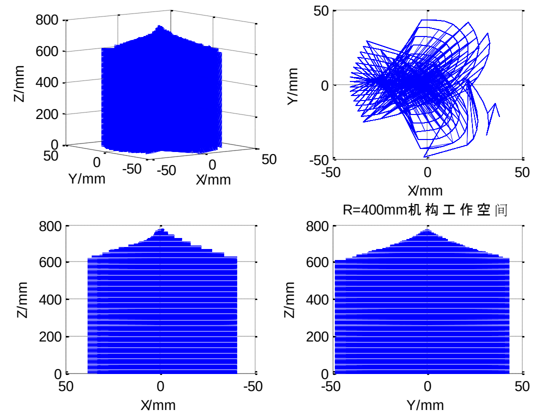

Figure 6. Working Space in $R=450mm$

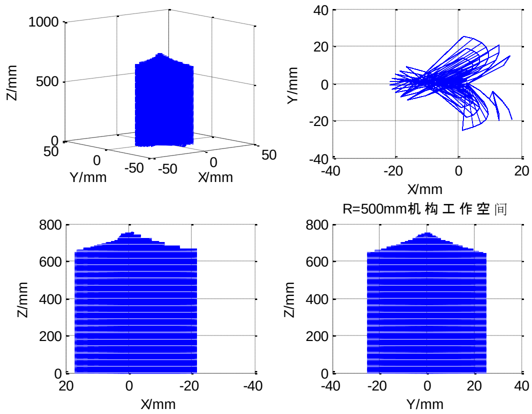

Figure 7. Working Space in $R = 500mm$

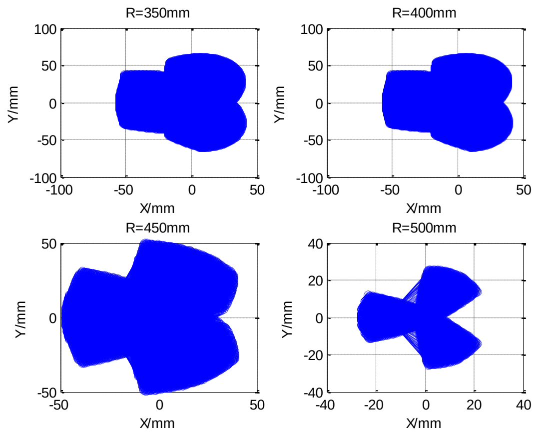

Figure 8. Working Space Projection on xoy Surface In Different Radius R

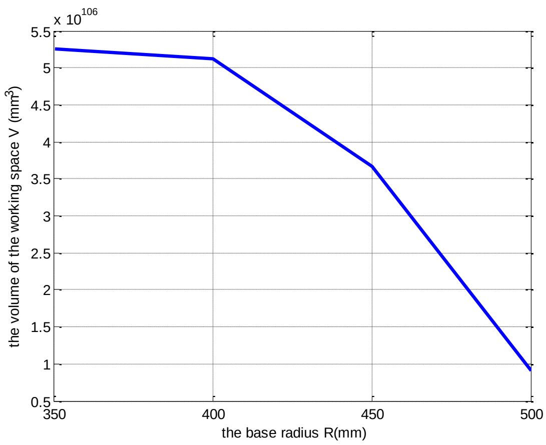

Figure 9. Volume of the Working Space in Different Radius R

Table 3 and Figure 4-Figure 9 show that the working space width on the x axis and y axis is gradually reduced, the working space height on the z axis is gradually reduced, and the volume of the working space is also gradually reduced. When R is relatively large, although the moving platform have a certain range of travel on the z axis, it has a weaker orientation-capability.

Influence of connecting rod length l on working space. The parameters of the mechanism are as follows: $r = 150mm$, $R_i = 350mm$ ($i = 1,2,3$) , $h = 20mm$. $l_1 = l_2 = l_3$, l values for 820mm, 850mm, 880mm and 910mm. Table 4 shows the working space width on the x axis and y axis, the working space height on the z axis and the volume of the working space. Figure 10-Figure 14 show the working space nephogram and projection on xoy, xoz and yoz surfaces.

Table 4. Influence of Connecting Rod Length l on Working Space

l (mm)	820	850	880	910
working space width on the x axis (mm)	86. 5031	86. 5031	86. 5031	86. 5031
working space width on the y axis(mm)	114.8175	114.8175	114.8175	114.8175
working space height on the z axis(mm)	807. 2	838.1	868. 9	899.7
volume of the working space (mm^3)	5. 2597×10^6	5.6378×10^6	5. 9635×10^6	6.2142×10^6

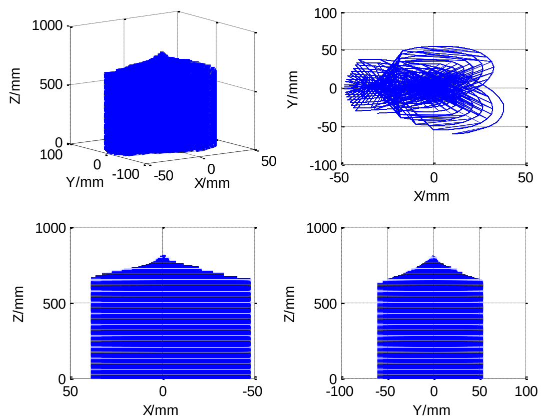

Figure 10. Working Space in $l = 820mm$

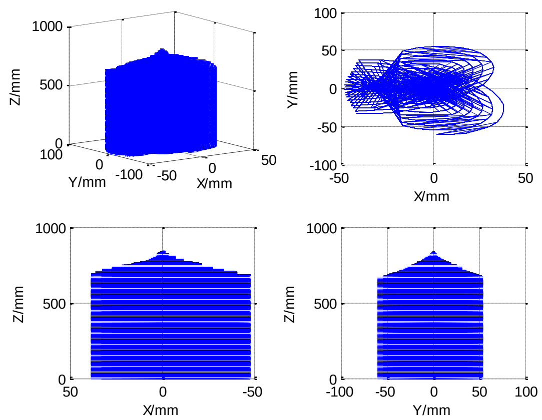

Figure 11. Working Space in $l = 850mm$

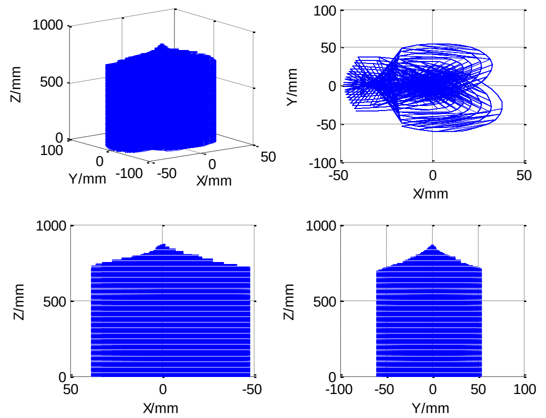

Figure 12. Working Space in $l = 880mm$

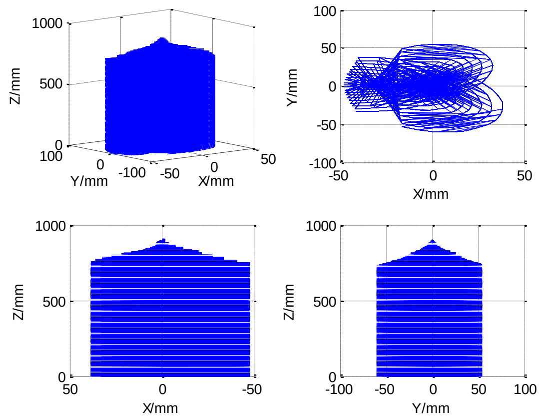

Figure 13. Working Space in $l = 910mm$

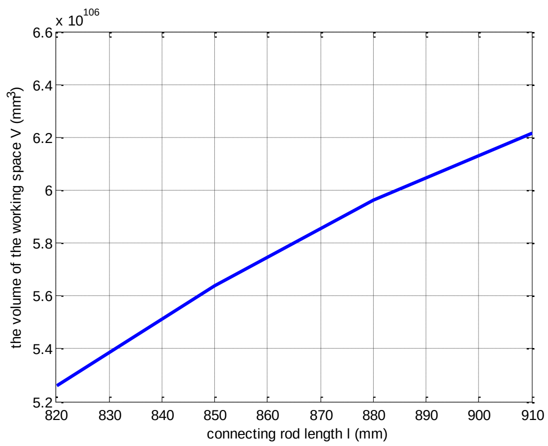

Figure 14. Volume of the Working Space in Different Connecting Rod Length l

Table 4 and Figure 10-Figure 14 show that the working space width on the x axis and y axis is unchanged, the height of the working space increases on the z axis, and the volume of the working space gradually increases. The projection of the working space does not change with connecting rod length ， on the xoy .In other words, the connecting rod length l has no influence on the orientation-capability of the mechanism, but it only affects the working space height on the z axis.

4. Conclusions

In this paper, a new type of 3-PRS parallel mechanism with adjustable working space is analyzed, and the mathematical model of the inverse kinematics is established. The main constraints which affect the motion of the mechanism are given, and the working space of the mechanism and the projection in Cartesian coordinate system are obtained by using the search algorithm in different conditions. The influence of the base radius and the connecting rod length on the working space is analyzed. From the results of the analysis, the following conclusions can be drawn:

(1) The working space of the 3-PRS parallel mechanism is symmetrical, which is consistent with its structural characteristics.

(2) With the increase of the base radius, the working space of the mechanism decreases gradually, and orientation-capability of 3-PRS parallel mechanism significantly decreases when R is relatively large.

(3) Connecting rod length l has no influence on the orientation-capability of the mechanism, it only affects the working space height on the z axis.

(4) This provides a theoretical basis for the optimal design of the mechanism.

Acknowledgments

This work is supported by Scientific and Technological Project of Henan Province of China with grant No.132102210430.The author would like to thank the anonymous reviewers for their valuable work. This paper is a revised and expanded version of a paper entitled [Workspace Analysis of a Novel 3-PRS Parallel Mechanism based on the Searching Method] presented at [ISI2016, Harbin, China and August 19-20, 2016].

References

[1] Y. Lu and B. Hu, “Development evaluation of limited-DOF parallel manipulators”, Journal of Yanshan University, vol.35, no. 5, **(2011)**, pp. 377-384.

[2] A. Peidró, A. Gil and J M. Marín, “A Web-based Tool to Analyze the Kinematics and Singularities of Parallel Robots”, Journal of Intelligent & Robotic Systems., vol.81, no. 1, **(2015)**, pp. 1-19.

[3] C. Brisan and A. Csiszar, “Computation and analysis of the workspace of a reconfigurable parallel robotic system”, Archives of Disease in Childhood, vol.32, no. 29, **(1993)**, pp. 7549-58.

[4] E. Macho, C. Pinto, E. Amezua and A. Hernández, “ Software Tool to Compute, Analyze and Visualize Workspaces of Parallel Kinematics Robots”, Advanced Robotics., vol.25, no. 6, **(2012)**, pp. 675-698.

[5] C. Wang, C. Gao, B. Chen and H. Wu, “Workspace Analysis and Structure Optimization of 3-RRR Spherical Parallel Mechanism”, Machinery Design & Manufacture., vol.4, no. 4, **(2015)**, pp. 55-58.

[6] H. Yun, X. Wang and S. Nian, “Workspace analysis and parameter optimization of 3-UrPS parallel mechanism”, Journal of Machine Design, vol.30, no. 11, **(2013)**, pp. 42-46.

[7] Z. Jin and X. He, “Workspace analysis of a novel 3-UPS parallel mechanism”, Journal of Yanshan University., vol.35, no. 3, **(2011)**, pp. 203-207.

[8] J. Fan, J. Cui and X. Zhu, “ Method of Solving Workspace of Planar Parallel Mechanism Drive by Angle Joint”, Journal of Mechanical Transmission., vol.4, no. 4, **(2013)**, pp. 77-79.

[9] Y. Zhang, Y. Zhang and X. Dai, “Optimal Design for Planar Cable-driven Parallel Mechanism with Respect to Maximizing Workspace”, Journal of Mechanical Engineering, vol.47, no. 13, **(2011)**, pp. 29-34.

[10] X. Chen, L. Chen and X. Liang, “Kinematics and Workspace Analysis of a Novel 4-DOF Redundant Actuation Parallel Mechanism”, Transactions of the Chinese Society for Agricultural Machinery, vol.45, no. 8, **(2014)**, pp. 307-313.

[11] S. Li, C. Yu and Y. Tian, “Kinematics analysis of a novel asymmetric four-DOF parallel mechanism”, Journal of Yanshan University, vol.35, no. 5, **(2011)**, pp. 385-390.

[12] B. Li, Y. Guo, C. Wang and Y. Cao, “Orientation workspace and global orientation capability analysis of the Gough-Stewart parallel mechanism”, Chinese Journal of Engineering Design, vol.5, no. 5, **(2015)**, pp. 452-460.

[13] J. Kand, G. Chen and J. Zhao, "Analysis on workspace of 3-PRS mechanism based on monte carlo method", Journal of Henan Polytechnic University (Natural Science), vol.33, no. 4, **(2014)**, pp. 478-481.
[14] J. Lei, Y. Cao and F. Wang, "Workspace Analysis of a 4UPS-UPU Parallel Mechanism Based on the Boundary Search Method", Machine Design & Research, vol.29, no. 1, **(2013)**, pp. 5-9.
[15] Y. Ji, H. Liu and D. Yuan, "Workspace and Scale Analysis of 4-SPS /PPU Parallel Mechanism", Transactions of the Chinese Society for Agricultural Machinery, vol.44, no. 11, **(2013)**, pp. 322-328.